A model for predicting the yield stress of AA6111 after multi-step heat treatments

B. Raeisinia[1], W.J. Poole[1], X. Wang[2] and D.J. Lloyd[3]

1. Dept. of Materials Engineering, The University of British Columbia, 309-6350 Stores Rd., Vancouver, BC, V6T 1Z4
2. Dept. of Materials Science and Engineering, McMaster University, 1280 Main St. W., Hamilton, ON, L8S 4L7
3. Novelis Global Technology Centre, P.O. Box 8400, Kingston, ON, K7L 5L9

Abstract

A model has been developed to predict the yield stress of the aluminum alloy AA6111 after multi-step heat treatments which involve combinations of ambient temperature ageing and high temperature artificial ageing. The model framework follows the internal state variable framework where the two principal state variables are i) the volume fraction of clusters which form at ambient temperature and ii) the volume fraction of metastable phases which form during high temperature ageing. The evolution of the these state variables has modeled using a set of coupled differential equations. The mechanical response (the yield stress) is then formulated in terms of the state variables through an appropriate flow stress addition law. To test the model predictions a series of experiments were conducted which examined two scenarios for multi-step heat treatments. In general, good agreement was observed between the model predictions and the experimental results. However, for the case where a short thermal excursion at 250 ^{o}C was applied immediately after the solution treatment, the results were not satisfactory.

This can be understood in terms of the importance of the temperature dependence for the nucleation density of metastable precipitates.

1. Introduction

Industrial processing of age hardening aluminum alloys often involves a complex thermal history where the material experiences a range of holding times at different temperatures with variable heating and cooling rates between processing temperatures, i.e. a highly non-isothermal situation. For example, in the use of automotive alloys, the thermal history may involve a solution heat treatment followed by ageing at ambient temperatures (so called natural ageing) combined with multiple high temperature (artificial) ageing steps which may involve different temperatures and times. It has been known for many years, that the ageing behaviour of these alloys is strongly history dependent [1,2] so that the development of an overall model becomes non-trivial. The simple example of this complexity arises when natural ageing proceeds artificial ageing and it is observed that the presence of the natural ageing step significantly delays the development of strength during subsequent high temperature ageing [1-5].

Esmaeili and co-workers have recently developed models to predict the limiting cases for isothermal artificial ageing of AA6111 either i) directly after solution treatment [6] or ii) after a combination of solution treatment and a variable period of ambient ageing [7]. The objective of the current work is to extend this model to the more general cases where combinations of ambient and artificial ageing steps are involved and where the effect of heating rate to the annealing temperature is explicitly accounted for. More specifically, the scope of the current model is to consider combinations of ambient

temperature ageing and artificial ageing at temperatures between 150 and 250 ^{o}C which involve final properties at or below the peak strength of the alloy, i.e. overaged conditions are not considered.

2. Model Development

Numerous recent studies have examined the complex precipitation sequence in 6000 series alloys [8]. The overall precipitation sequence for copper containing alloys can be described as [9]:

SSS → clusters/GP zones → β" + precursor of Q → equilibrium Q + Mg_2Si

At ambient temperatures, the precipitation reaction is dominated by formation of co-clusters of Mg, Si and Cu atoms as has been illustrated in the atom probe work of Vaumouse et al. [10] and Murayama et al. [11,12]. At high temperatures, considerable controversy exists regarding the initial stages of ageing and the role of GP zones, however, after a very short times (e.g. 15 minutes at 180 C) strengthening is dominated by the formation of the metastable *β"* and the precursor of Q phases [13,14]. In the current work, it is assumed that the clustering reaction dominates for ambient temperature ageing and that for ageing at temperatures between 150 and 250 ^{o}C, precipitation is dominated by the formation of the *β"* and precursor of *Q* phases, predominately the *β"* phase.

The current modelling framework follows the internal state variable approach [15-17]. In this framework, the material response, X_i, is a function of the internal state variables, S_1, S_2, S_3 … etc. which represent the microstructure, i.e.:

$$X_i = g(S_1, S_2, ...) \tag{1}$$

These state variables evolve with time and thus, their evolution can be written as a series of linked differential equations:

$$\frac{dS_1}{dt} = h_1\left(T, S_1, S_{2,}...\right) \tag{2a}$$

$$\frac{dS_2}{dt} = h_2\left(T, S_1, S_{2,}...\right) \tag{2b}$$

etc., where T is the temperature.

In the present work , the material response of interest is the yield stress, σ_{ys}, and the relevant internal state variables are the volume fraction of clusters, $f_{cluster}$, and the volume fraction of metastable precipitates, f_{ppt},[1]. Further, it is convenient to write these two variables in a normalized form, i.e.

$$f_{r_{clusters}} = \frac{f_{clusters}}{f^*_{clusters}} \tag{3a}$$

and

$$f_{r_{ppt}} = \frac{f_{ppt}}{f^*_{ppt}} \tag{3b}$$

where $f^*_{clusters}$ and f^*_{ppt} are the volume fraction of clusters and precipitates when the peak strength of the alloy is reached for ageing at ambient temperature and ageing at elevated temperatures, respectively.

The advantage of formulating this problem in this framework is that highly non-isothermal processing routes can easily and explicitly modeled using this approach. Therefore, one can include the effect of heating rate to temperature (which is of particular

[1] Note: f_{ppt}, represents the sum of the metastable β" and precursor of Q phases.

importance for short high temperature thermal excursions) and one can also examine multi-step heat treatments which are commonly observed in industrial processes.

2.1 - Evolution of clusters

The work of Panseri and Federighi [18]and Kelly and Nicholson [18,19] has shown that the clustering reaction at ambient temperatures occurs in two stages, i.e. rapidly at first when the excess vacancy concentration is high and then at a slower rate. Empirically this evolution can be captured using an Avrami evolution law [7]. In differential form, this can be written as:

$$\frac{df_{r_{cluster}}}{dt} = n_1 k_{cluster}^{1/n_1} \left(1 - f_{r_{cluste}}\right) \cdot \left[\ln \frac{1}{1 - f_{r_{cluster}}}\right]^{\frac{n_1 - 1}{n_1}} \tag{4}$$

where n_1 and $k_{cluster}$ are fitting parameters which describe the evolution of clusters. However, there is a further complication since the clustering reaction is strongly dependent on the level of supersaturated solutes available for cluster formation. For example, if high temperature ageing precedes ambient temperature ageing, then depending on the solute consumed in the high temperature reaction, cluster formation will be reduced or may even be eliminated. This accounted for by assuming that the kinetic parameter, $k_{cluster}$, is a function of the fraction of precipitates formed in the preceding steps of the heat treatment, i.e.

$$k_{clusters} = k^*_{cluster} \left(1 - \alpha_1 f_{r_{ppt}}\right) \tag{5}$$

where $k^*_{clusters}$ describes the kinetics of cluster formation for the case of ambient temperature ageing immediately after solution treatment. The magnitudes for n_1 and $k^*_{clusters}$ were determined by Esmaeili et al (note: for values of $\alpha_1 f_{r_{ppt}} > 1$ then $k_{cluster}$ =

0). By writing equation (4) in differential form, it allows one to easily keep track of the volume fraction of clusters for multi-step ageing treatments.

For ageing of solution treated materials at temperatures in the range of 150- 250 ^{o}C, the clustering reaction is either very quick or may even not occur and therefore can be ignored. However, if clusters have formed by a previous ambient temperature ageing step, the clusters will dissolve or revert in this temperature range. It has been shown that the dissolution of clusters can be captured by a diffusion controlled model [7], i.e.

$$\frac{df_{r_{clusters}}}{dt} = -\frac{3}{2}B^2 \frac{\left(f_{r_{clusters}}\right)^{2/3}}{1-\left(f_{r_{clusters}}\right)^{1/3}} \tag{6}$$

where B is a temperature dependent parameter to describe the dissolution kinetics. The temperature dependence of B can be described by an Arrenhius relationship, i.e.

$$B = B_o \exp\left(\frac{-Q_{dis}}{RT}\right) \tag{7}$$

where B_o is a constant and Q_{dis} is the activation energy for cluster dissolution.

2.2 - Precipitate Formation (20-250 ^{o}C)

To a first approximation, Esmaeili et al. showed that by using an isothermal calorimetry technique the kinetics for the formation of metastable precipitates during artificial ageing could also be well described by an Avrami equation [6,7]. In differential form, this can be written as:

$$\frac{df_{r_{ppt}}}{dt} = n_2 k_{ppt}^{1/n_2}\left(1-f_{r_{ppt}}\right)\cdot\left[\ln\frac{1}{1-f_{r_{ppt}}}\right]^{\frac{n_2-1}{n_2}} \tag{8}$$

where k_{ppt} and n_2 are constants which describe the kinetics of precipitation for the metastable precipitates. The constant k_{ppt} is a function of both temperature and the fraction of clusters present at the beginning of the artificial ageing step. Esmaeili et al showed that the kinetic parameter k_{ppt} for the limiting cases of artificial ageing after solution treatment (k_{ST}) and artificial ageing after ambient ageing times greater than 1 day (k_{NA})are given by:

$$k_{ST} = k_{o(ST)} \exp\left(\frac{-Q_{ST}}{RT}\right) \tag{9a}$$

and

$$k_{NA} = k_{o(NA)} \exp\left(\frac{-Q_{NA}}{RT}\right) \tag{9b}$$

where $k_{o(ST)}$ and $k_{o(NA)}$ are constant while Q_{ST} and Q_{NA} are the activation energies for the precipitation reaction for solution treated and ambient aged materials, respectively. To account for a smooth transition between these limiting cases, it is proposed that k_{ppt} may be written as:

$$k_{ppt} = k_{NA} + \left(k_{ST} - k_{NA}\right)\exp\left(-\alpha_2 f_{r_{cluster}}\right) \tag{9c}$$

where the parameter α_2 is an adjustable parameter which characterizes the transition between the two limiting cases.

2.3 - Mechanical Response (Yield Stress)

The yield stress of the material can now be estimated by assembling the various contributions [6,7]. The contribution to the yield stress from cluster strengthening can be written as:

$$\sigma_{clusters} = C_1 \left(f_{r_{cluster}} \right)^{1/2} \tag{10}$$

where C_1 is a constant. Further, the contribution from precipitation hardening is given by:

$$\sigma_{ppt} = C_2 \left(f_{r_{ppt}} \right)^{1/2} \tag{11}$$

where C_2 is a constant. Finally, solid solution strengthening is determined from a mass balance, i.e. the residual solid solution content accounting for the loss of solute to clusters and precipitates.

$$\sigma_{ss} = C_3 \left(1 - f_{r_{cluster}} - f_{r_{ppt}} \right)^{2/3} \tag{12}$$

where C_3 is a constant.

The overall yield strength is obtained by an appropriate summation of the flow stress contributions. In this case, the cluster and precipitate contributions are obtained by summing the densities of these two types of obstacles and since the density of obstacles is proportional to the square of the flow stress contributions, a Pythagorean addition law is appropriate:

$$\sigma_{ys} = \sigma_i + \sigma_{ss} + \left(\sigma_{cluster}^2 + \sigma_{ppt}^2 \right)^{1/2} \tag{13}$$

2.4 - Calibration and Implementation of Model

The necessary parameters for implementation of the model are summarized in Table 1. With the exception of the parameters α_1 and α_2 , all the necessary constants were obtained in the work of Esmaeili et al. [6,7] by fitting of isothermal annealing experiments on solution treated and naturally aged materials. The parameter α_1 has been

added via equation (5) to account for the effect of precipitate formation on subsequent natural ageing (i.e. if precipitates form during a high temperature ageing step, this will remove solutes from the matrix and thereby inhibit cluster formation during subsequent ambient ageing steps). The overall model results are relatively insensitive to the exact value of α_1.

It was also necessary to introduce one additional constant to capture the transition in the artificial ageing kinetics as a function of the fraction of clusters that have formed during previous ambient ageing steps. Equation (9) allows for a smooth transition between the limiting cases, i.e. when there is no ambient ageing prior to artificial ageing ($f_{r_{clusters}}$ =0) and when ambient ageing produces the maximum number of clusters ($f_{r_{clusters}}$). Again, the model results were relatively insensitive to the value of α_2 in equation (9).

Finally, the differential equations (4, 6 and 8) were numerically integrated over the temperature-time history of the multi-step ageing treatment (including the heating rate to the artificial ageing temperature which had been characterized experimentally). The current value of the state variables was calculated as for example:

$$f^{\,i}_{r_{clusters}} = f^{\,i-1}_{r_{clusters}} + \frac{df_{r_{clusters}}}{dt}\Delta t$$

The magnitude of the time step, Δt, used in the spread sheet was determined by trial and error, i.e. the time step was reduced until further reductions in the time step did not affect the solution.

3.0 Comparison of Model and Experiments for multi-step ageing treatments

In order to test the predictions of the model, a series of multi-step ageing experiments which involved combinations of ambient temperature ageing, a low artificial ageing temperature (180 ^{o}C) and a short thermal excursion to a higher artificial ageing temperature (either 220 or 250 ^{o}C) was utilized. The philosophy for choosing the experiments was to examine two basic scenarios. In scenario A, the material was exposed to a short thermal excursion (30, 60 or 300 s) at either 220 or 250 ^{o}C immediately following the solution treatment with the objective of precipitating a sufficient amount of metastable precipitates such that clustering would be prevented during a subsequent ambient temperature period of 1 day. After this ambient temperature ageing period, the material was aged at 180 ^{o}C for 30 minutes and 7 hours (previously determined time to reach the peak strength at 180 ^{o}C). In scenario B, the material was aged at ambient temperature for 2 weeks to allow for substantial cluster formation and then exposed to a short thermal excursion (30, 60 or 300 s) at either 220 or 250 ^{o}C with the objective of dissolving the clusters and precipitating the metastable precipitates such that the material would be stable against subsequent cluster formation during ambient temperature ageing. After an ambient temperature ageing of 1 day, these materials were finally annealed at 180 ^{o}C for up to 7 hours. Figure 1 schematically illustrates the two scenarios that have been examined in this work..

The material used in this study was provided by Novelis from an industrial processing line. The chemistry of the alloy in weight percent was 0.8Mg, 0.6Si 0.7Cu, 0.25 Fe and 0.2 Mn. Annealing treatments (solution treatment and artificial ageing) for temperatures above 200 ^{o}C were done in salt baths (for annealing at 180 ^{o}C, a high temperature oil bath was used). A thermocouple was spot welded on sample to measure

the temperature of the sample during the heating and hold period. Typically, the experimentally determined average heating rate was 40-50 ^{o}C/s. The yield stress of the material was determined by conducting standard tensile tests using a MTS servo-hydraulic test machine. The yield stress was characterized by 0.2% offset method.

3.1 – Results for Scenario A

Figure 2a compares the results from the experiments with the model predictions for scenario A where the thermal excursion temperature was 220 ^{o}C. Turning first to the predictions of the yield stress after the thermal excursion, one can observe that the model gives reasonable predictions. The model gives a small over prediction of the yield stress for excursion times of 30 and 60 s but slightly under predicts the yield stress after 300 s. After the thermal excursion, the sample was held at ambient temperature for 1 day. Figure 3a illustrates the change in the yield stress following ambient ageing temperature from the experiments and the model predictions. It can be observed that for excursion times greater than or equal to 60 s, both the model and experiments show no change in yield stress. For an excursion time of 30 s, there was a change in yield stress (which is indirect evidence of clustering)**.** Returning to Figure 2a, one can compare the model predictions for the final ageing step at 180 ^{o}C. For both 30 minutes and 7 hours at 180 ^{o}C, the model and experiments are in good agreement (within 5 % for excursions of 30, 60 and 300 s).

Figure 2b summarizes the results for scenario A where the thermal excursion temperature was 250 ^{o}C. In this case, there are significant discrepancies between the model predictions and the experimental results. Specifically, after the thermal excursion, the model over predicts the yield stress in the worst case (i.e. 300 s) by more than 25 %.

Furthermore, as shown in Figure 3b, there is a significant difference between the model predictions and experimental values for the change in yield stress during ambient temperature ageing following the excursion, i.e. the model predicts no change in yield stress while the experiments show evidence of natural ageing. Continuing along the thermal path, one can observe that the model also strongly over predicts the magnitude of the yield stress following ageing for 30 minutes at 180 ^{o}C. However, after 7 hours at 180 ^{o}C the model predictions and experimental results converge suggesting that the peak strength is relatively insensitive to the thermal history for this alloy. The possible reasons for these discrepancies will be considered in Section 4.

3.2 – Results for Scenario B

Figure 4a compares the results for the case of 2 weeks of ambient temperature followed by a thermal excursion to 220 ^{o}C. In this case, substantial dissolution of the clusters which formed at ambient temperature occurs concurrently with the precipitation of metastable precipitates (although the rate of this precipitation is greatly reduced *viz.* material which experiences a thermal excursion immediately after the solution treatment). One can observe that there is good agreement between the model predictions for the yield stress after the thermal excursion and the experimental results. After the thermal excursion, the samples were held at ambient temperature for 1 day. In this case, little or no change in the yield stress occurred during this period, suggesting that the clustering reaction had been suppressed. It was observed that the subsequent ageing at 180 ^{o}C was predicted well by the model although for the combination of the 5 minute thermal excursion and 30 minutes at 180 ^{o}C, the model slightly over predicted the experimental result. While the experiments only give information on the evolution of the overall yield

strength, it is possible to track the individual components of the yield stress using the model. Figure 5 summarizes the evolution of solid solution, cluster and precipitation hardening contributions to the yield stress for this scenario, i.e. thermal excursions of 60 and 300s. It can be observed i) cluster formation during ambient temperature ageing, ii) partial cluster dissolution during thermal excursion for 60 s and complete dissolution for 300 s, iii) the absence of cluster formation during ambient ageing after thermal excursion and iv) the precipitation of the metastable precipitates (here we see that the kinetics are faster when the clusters are completely dissolved).

Finally, Figure 4b compares the results for the case of two weeks of ambient temperature ageing followed by a thermal excursion to 250 ^{o}C, 1 day at ambient temperature and then artificial ageing at 180 ^{o}C. In this case, there is good qualitative and quantitative agreement between the model and experiments. One sees that both the model and the experiments show a drop in the yield stress for short thermal excursions due to the dissolution of clusters. With increasing time of the thermal excursion, the yield stress of the material increases due to substantial precipitation of the high temperature metastable precipitates. For this case, neither the experiments nor the model suggest that cluster formation is significant during ambient temperature ageing following the thermal excursion. The model also gives very good predictions for the evolution of the yield stress during the final artificial ageing step at 180 ^{o}C as shown in Figure 4b.

4.0 Discussion

Overall, the predictions of the proposed model are in good agreement, both qualitatively and quantitatively, with the experimental observations. Qualitatively, the model is able to track cluster formation during ambient temperature ageing either directly

after the solution treatment or after a short thermal excursion. In addition, for elevated temperature ageing of materials with initial volume fraction of clusters, the model tracks the dissolution of these clusters and the concurrent precipitation of the metastable precipitates which gives rise to hardening. Figure 6 summarizes a comparison of the model predictions with the experimental results for all conditions examined in this work, i.e. after the thermal excursion, after ambient temperature ageing steps and after ageing for either 30 minutes or 7 hours at 180 ^{o}C. A close examination of the results indicates that for scenario A and B where the thermal excursion temperature was at 220 ^{o}C, there is excellent agreement between the model and experiments, i.e. there is a difference of less than ±10 % for all conditions examined as shown in Figure 6. The situation was different for thermal excursions at 250 ^{o}C. This is, perhaps, not too surprising since this involved extrapolating the models of Esmaeili et al. outside the range for which their model had been validated (i.e the models had been validated between 160 and 220 ^{o}C). Nevertheless, for scenario B (thermal excursion after ambient temperature ageing), good predictions are found except for the initial points immediately after the thermal excursions where the model slightly over predicts the yield stress. However, for the case where a thermal excursion at 250 ^{o}C immediately follows the solution treatment (scenario A), the model consistently over predicts the yield stress by 20-25 %.

The reasons for the discrepancies in the model predictions can be understood by examining the precipitation state for ageing of the solution treated material at different ageing temperatures. Figure 7 illustrates dark field transmission electron microscope (TEM) images for samples aged to the peak strength at 180 and 250 ^{o}C. Qualitatively, the sample aged at 180 ^{o}C has a much a finer scale of precipitation compared to the

sample aged at 250 ^{o}C. Wang et al. have measured the number density of the precipitates to be 88.7 x 10^{21} m^{-3} and 6.4 x 10^{21} m^{-3} for peak aged at 180 and 250 ^{o}C, respectively [13,14]. Furthermore, Wang et al. showed that for ageing at 180 ^{o}C more than 80 % of the precipitate population was β" while for ageing at 250 ^{o}C the fraction of β" dropped to less than 60 % of the population. While these observations refer to the scale of the microstructure at the peak aged condition, Wang et al. have shown that within a factor of two, this is a good approximation of the maximum number density of precipitates observed. Thus, this can be used as an estimate of the nucleation density.

There are two important implications to the coarse precipitate structure observed when ageing at 250 ^{o}C. First, the diameter of precipitates is large enough that mobile dislocations will by-pass the particles rather than shearing [9]. For this case, precipitation hardening will scale with the interparticle spacing on the slip plane. This results in a lower strengthening response. For example, the samples shown in Figure 7 have peak aged yield stresses of 340 and 255 MPa for ageing conditions of 180 and 250 ^{o}C, respectively [14]. This would explain why the model of Esmaeili et al. which assumes finely spaced shearable precipitates used in this work over predicts the experimental results. The second effect of having such a coarse precipitate distribution is that the impingement of diffusion field during growth is delayed [20]. This may be of particular importance for short ageing times at 250 ^{o}C resulting in regions between the precipitates which are highly supersaturated in solute and therefore may experience clustering during subsequent ambient temperature ageing. This would explain why the experiments show a substantial increase in yield stress during ambient temperature ageing after the short thermal excursions to 250 ^{o}C as shown in Figure 3b.

5.0 Conclusions

A model for the yield stress evolution during multi-step heat treatments on the aluminum alloy AA6111 has been proposed. Very good agreement is observed between the model and the experiments when the multi-step ageing treatments involved thermal excursions at 220 ^{o}C. The model is able to predict the evolution of yield stress throughout the multi-step ageing treatment and therefore provide insight not only into the strength of the material but also the evolution of microstructure. The situation was more complex for the cases which included thermal excursions to 250 ^{o}C. If the thermal excursion followed ambient temperature ageing, good agreement was observed. However, if the thermal excursion immediately followed the solution treatment, then the results of the model were unsatisfactory. This was shown to be related to the coarse scale of precipitation observed under these conditions. For this case, it is clear that the simple precipitation model used in this work is no longer satisfactory and it is, therefore, necessary to consider the complex problem of nucleation for the metastable precipitates and the interaction of this process with the clustering reaction. This is a challenging problem which requires a combination of careful experimental work and the development of a fundamental nucleation, growth and coarsening model (e.g. see Myhr and Grong [21,22]) which could then be linked to a yield stress model such as proposed by Wang et al. for AA6111 [14]. The overall model framework proposed here would still be appropriate but the evolution laws would be considerably more complicated and it would be necessary to explicitly account for the formation of both the the was β" and precursor to *Q* phases.

Acknowledgements

The authors would like to acknowledge the financial support of NSERC Canada which made this work possible.

Table 1

Parameter	Value
α_1	6.5
α_2	25
B_0	$1.08\times10^{8}\ s^{-1/2}$
$C1$	320 MPa
$C2$	160 MPa
$C3$	50 MPa
$k_{0(NA)}$	$1.04\times10^{7}\ s^{-1}$
$k_{0(ST)}$	$3280\ s^{-1}$
$k^{*}_{clusters}$	$0.02\ h^{-1/2}$
n_1	½
n_2	1
Q_{dis}	88 kJ/mol
Q_{NA}	95 kJ/mol
Q_{ST}	58 kJ/mol
σ_i	10 MPa

List of Figures

References

1. D.W. Pashley, J.W. Rhodes, A. Sendorek, *J. Inst. Met*, 1966, vol. 94, pp. 41-49.
2. D.W. Pashley, M.H. Jacobs, J.T. Vietz, *Phil. Mag.*, 1967, vol. 16, pp. 51-76.
3. D.J. Lloyd, *Mater. Forum*, 2004, vol. 28, pp. 107-117.
4. W.J. Poole, D.J. Lloyd, J.D. Embury, *Mat. Sci. Eng.*, 1997, vol. A234-236, pp. 306-309.
5. D.J. Lloyd, D.R. Evans, A.K. Gupta, *Can. Met. Quart.*, 2000, vol. 39, pp. 475-482.
6. S. Esmaeili, D.J. Lloyd, W.J. Poole, *Acta mater.*, 2003, vol. 51, pp. 2243-2257.
7. S. Esmaeili, D.J. Lloyd, W.J. Poole, *Acta mater.*, 2003, vol. 51, pp. 3467-3481.
8. D.J. Chakrabarti, D.E. Laughlin, *Prog. Mat. Sci.*, 2004, vol. 49, pp. 389-410.
9. W.J. Poole, X. Wang, D.J. Lloyd, J.D. Embury, *Phil. Mag.*, 2005, vol.??, pp. in press.
10. D. Vaumousse, A. Cerezo, P.J. Warren, S.A. Court, *Mat. Sci. For.*, 2002, vol. 396-402, pp. 693-698.
11. M. Murayama, K. Hono, *Acta mater.*, 1999, vol. 47, pp. 1537-1548.
12. M. Murayama, K. Hono, W.F. Miao, D.E. Laughlin, *Metall. Mater. Trans. A.*, 2001, vol. 32A, pp. 239-246.
13. S. Esmaeili, X. Wang, D.J. Lloyd, W.J. Poole, *Metall. Mater. Trans. A.*, 2003, vol. 34A, pp. 751-763.
14. X. Wang, W.J. Poole, S. Esmaeili, D.J. Lloyd, J.D. Embury, *Metall. Mater. Trans. A.*, 2003, vol. 34A, pp. 2913-2924.
15. O. Richmond, *J.Metals*, 1986, vol. 38, pp. 16-18.
16. O. Grong, H.R. Shercliff, *Prog. Mat. Sci.*, 2002, vol. 47, pp. 163-282.
17. W.J. Poole, H.R. Shercliff, T. Castillo, *Mat. Sci. Tech.*, 1997, vol. 13, pp. 897-904.
18. C. Panseri, T. Fegerighi, *J. Inst. Met*, 1966, vol. 94, pp. 99-107.
19. A. Kelly, R.B. Nicholson, *Prog. Mat. Sci.*, 1963, vol. 10, pp. 312-315.
20. S. Esmaeili, private communication.
21. O.R. Myhr, O. Grong, *Acta mater.*, 2000, vol. 48, pp. 1605-1615.
22. O.R. Myhr, O. Grong, S.J. Anderson, *Acta mater.*, 2001, vol. 49, pp. 65-75.

Figures

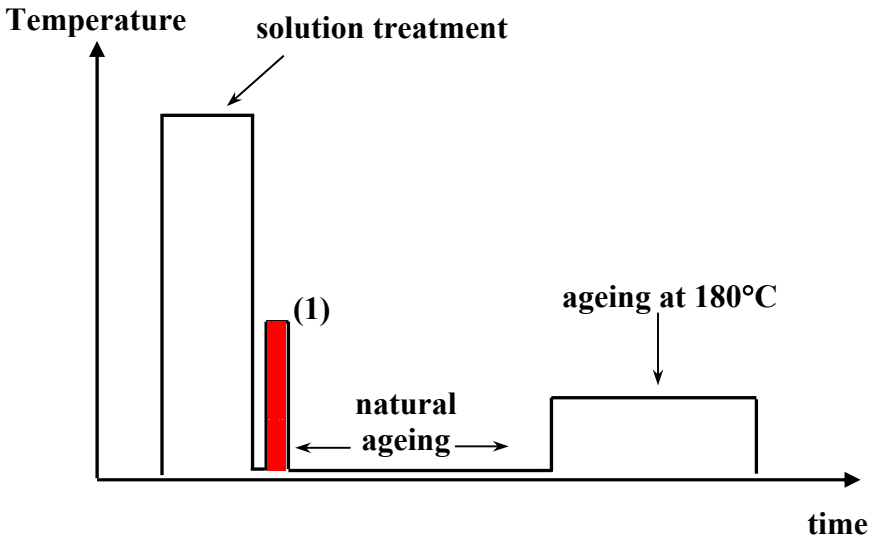

(a) Scenario A

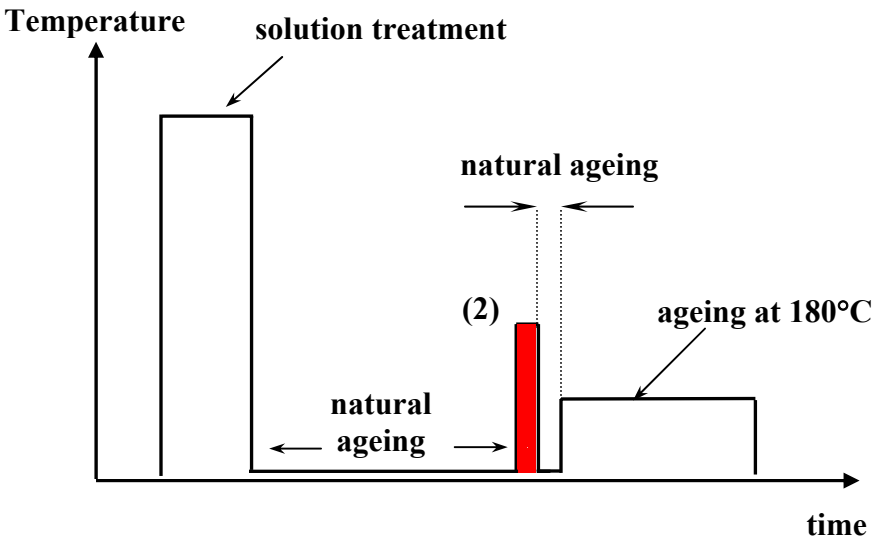

(b) Scenario B

Figure 1 – Schematic diagram illustrating the two multi-step heat treatment scenarios that were used to test the model predictions.

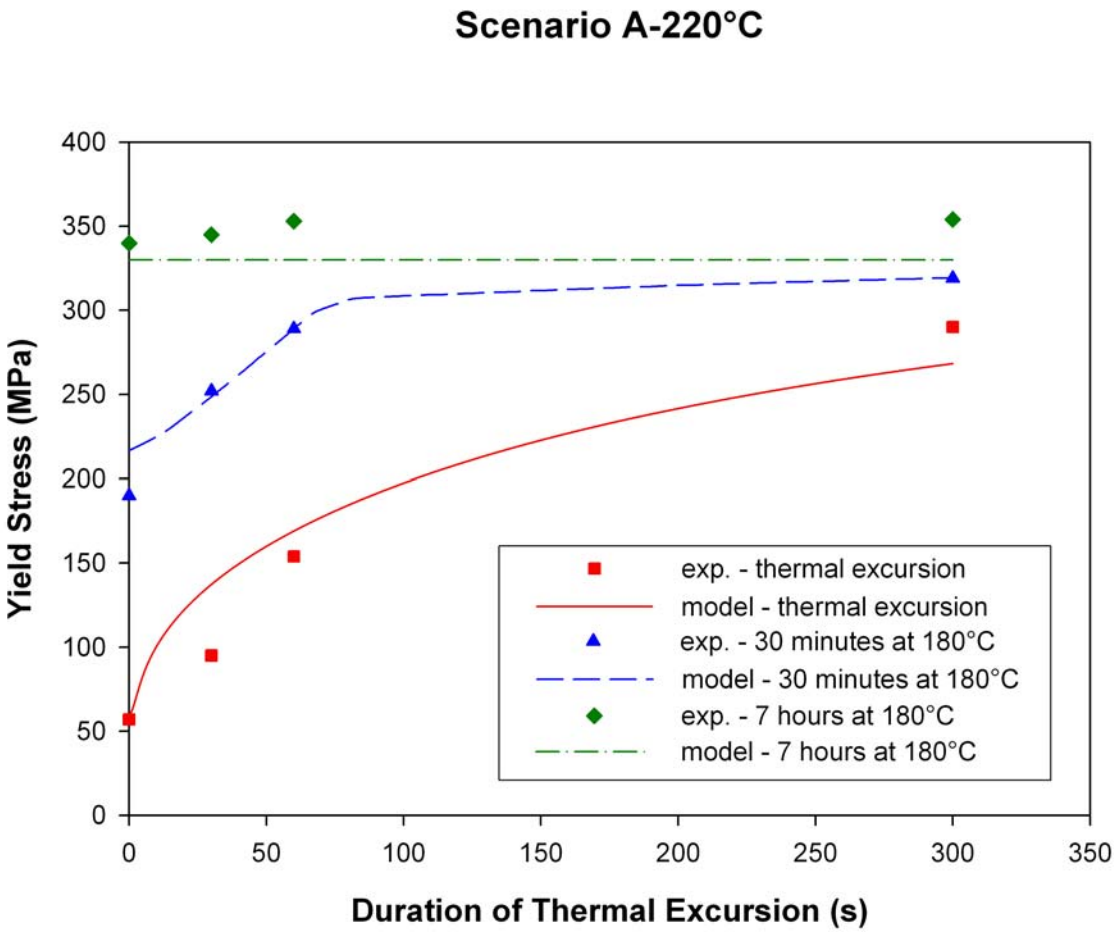
Scenario A-220°C
Yield Stress (MPa)
Duration of Thermal Excursion (s)
0
50
100
150
200
250
300
350
400
exp. - thermal excursion
model - thermal excursion
exp. - 30 minutes at 180°C
model - 30 minutes at 180°C
exp. - 7 hours at 180°C
model - 7 hours at 180°C

Figure 2a

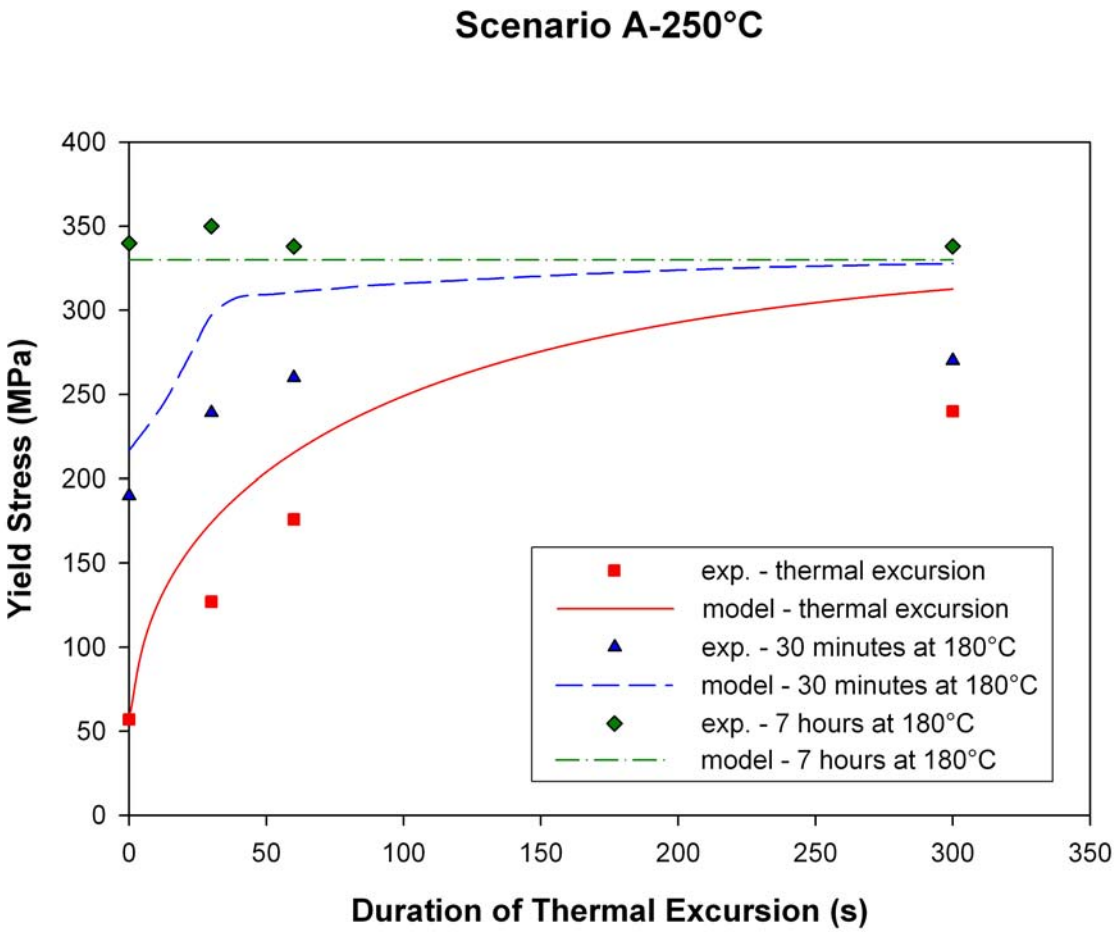

Figure 2b

Figure 2 – Comparison of the model prediction with experimental yield stresses for heat treatment scenario A as a function of the duration of the thermal excursion. a) thermal excursion at 220 ^{o}C and b) thermal excursion at 220 ^{o}C. Note: "thermal excursion" refers to the yield stress after the thermal excursion.

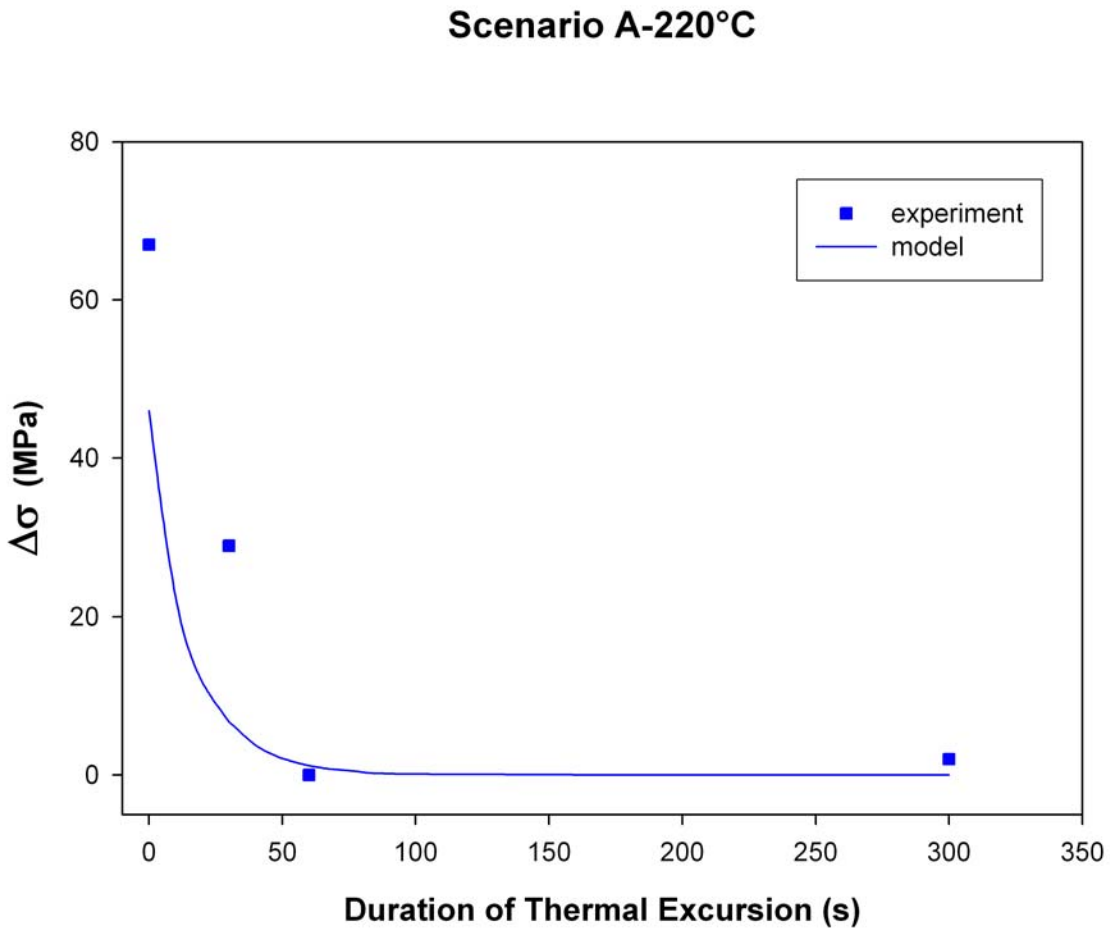
Scenario A-220°C
80
60
40
20
0
Δσ (MPa)
0
50
100
150
200
250
300
350
Duration of Thermal Excursion (s)
experiment
model

Figure 3a

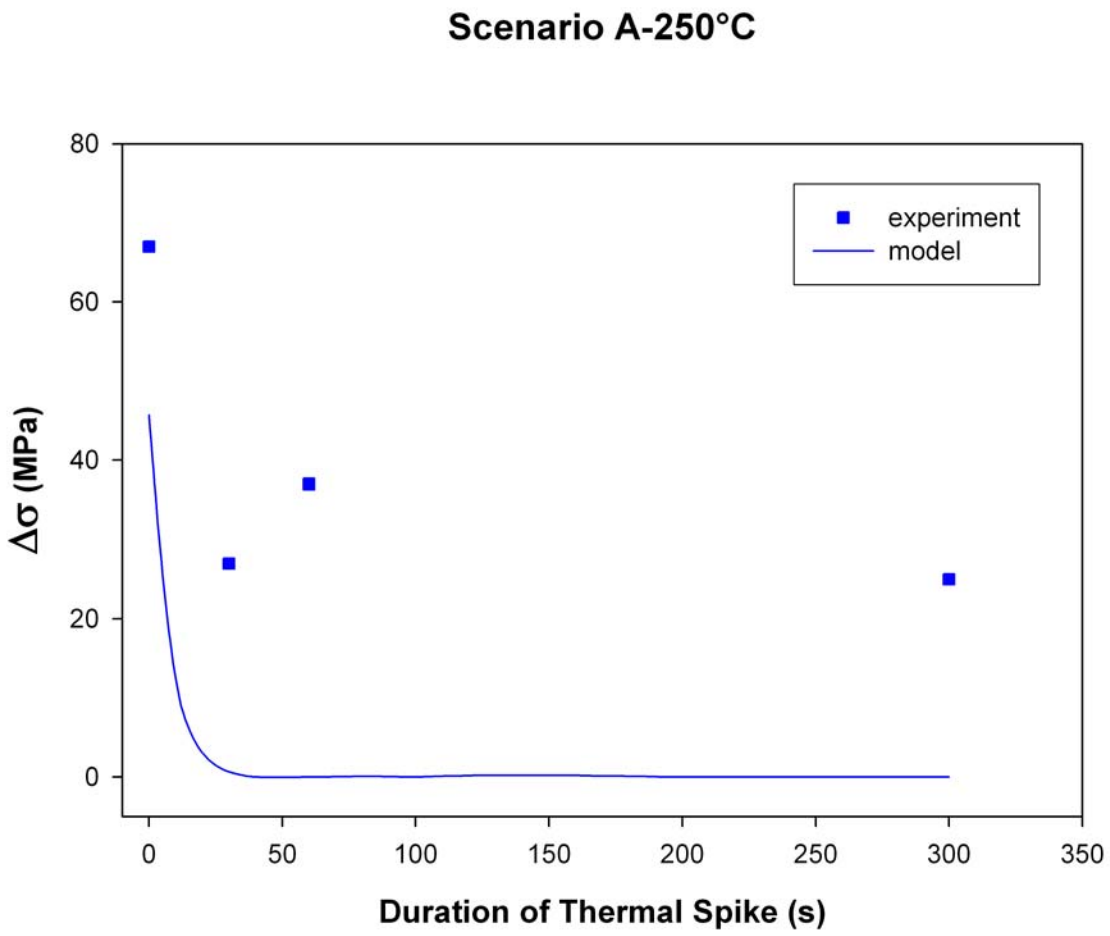

Figure 3b

Figure 3 – The change in yield stress during the ambient ageing step after the thermal excursion in scenario A as a function of the duration of the thermal excursion. . a) thermal excursion at 220 ^{o}C and b) thermal excursion at 220 ^{o}C.

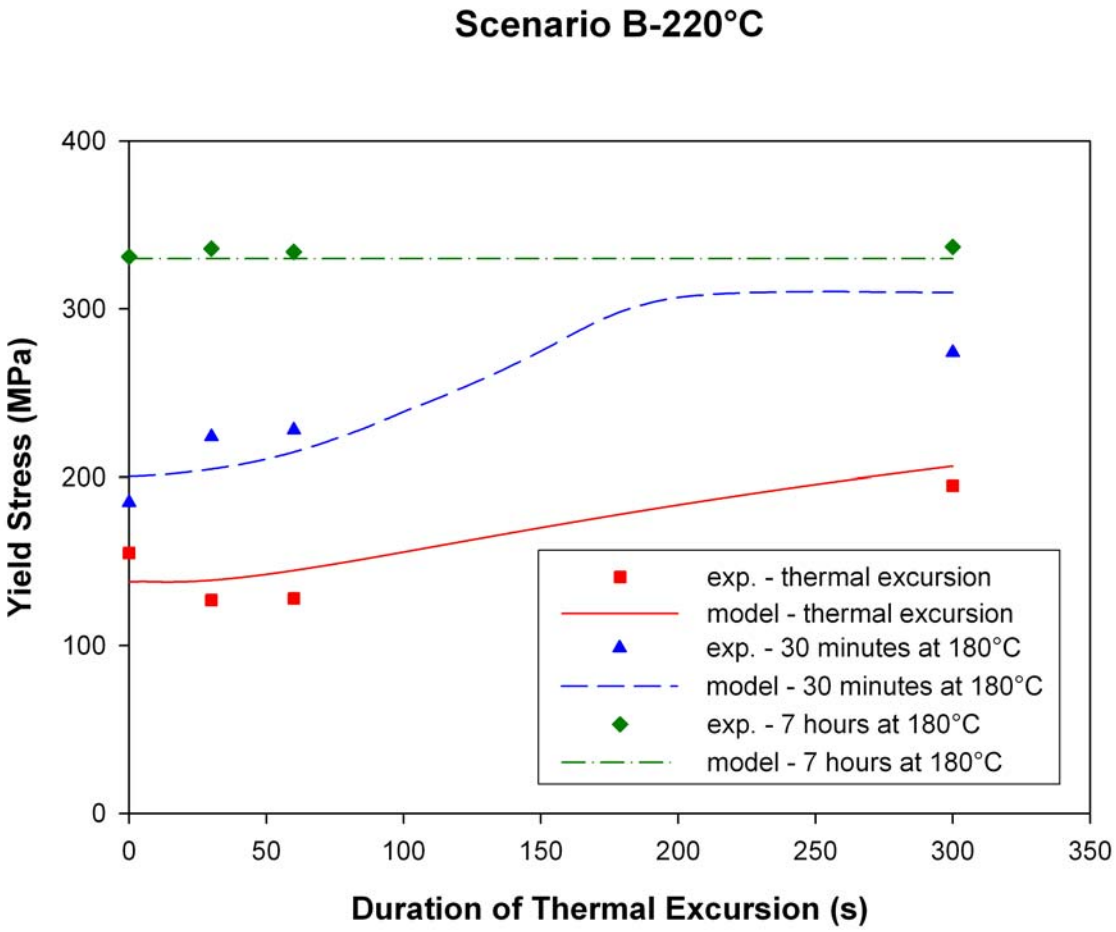
Scenario B-220°C
Yield Stress (MPa)
Duration of Thermal Excursion (s)
0
100
200
300
400
0
50
100
150
200
250
300
350
exp. - thermal excursion
model - thermal excursion
exp. - 30 minutes at 180°C
model - 30 minutes at 180°C
exp. - 7 hours at 180°C
model - 7 hours at 180°C

Figure 4a

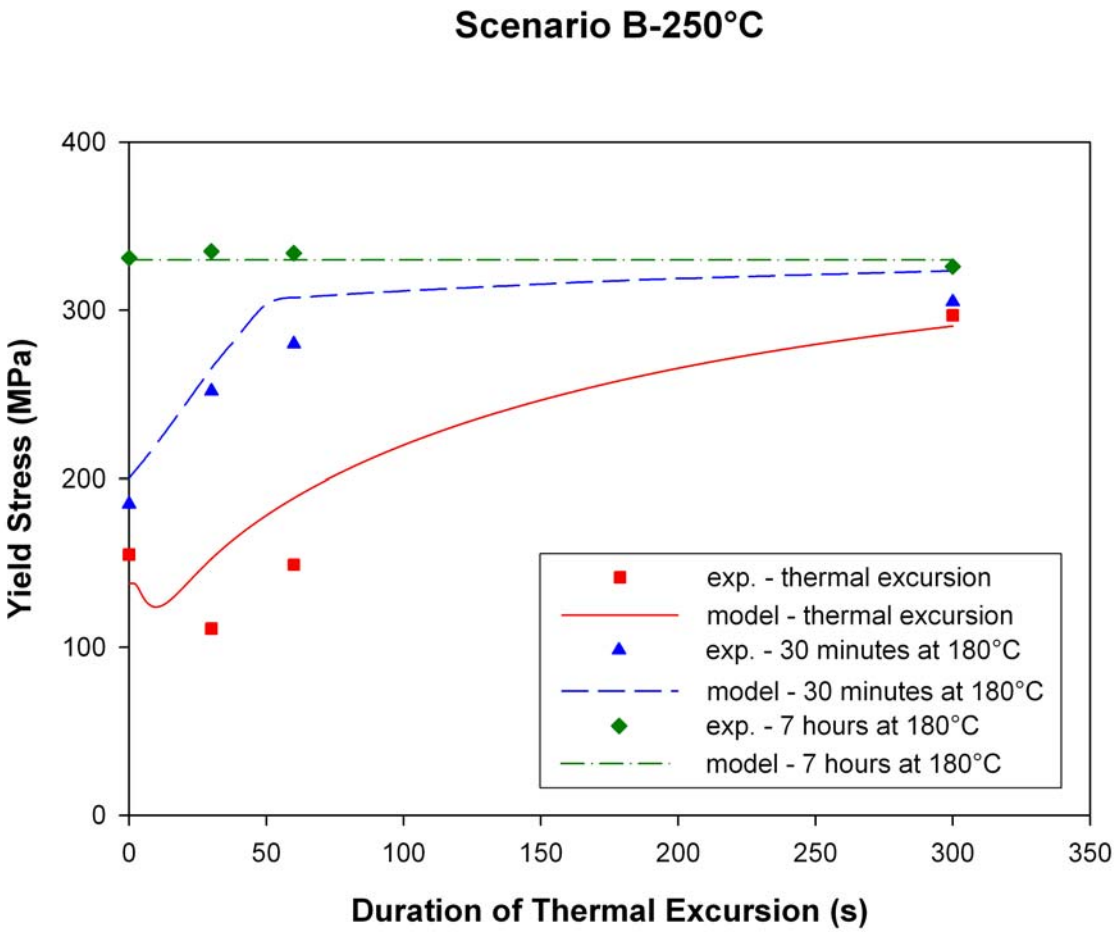

Figure 4b

Figure 4 – Comparison of the model prediction with experimental yield stresses for heat treatment scenario B as a function of the duration of the thermal excursion. a) thermal excursion at 220 ^{o}C and b) thermal excursion at 220 ^{o}C. Note: "thermal excursion" refers to the yield stress after the thermal excursion.

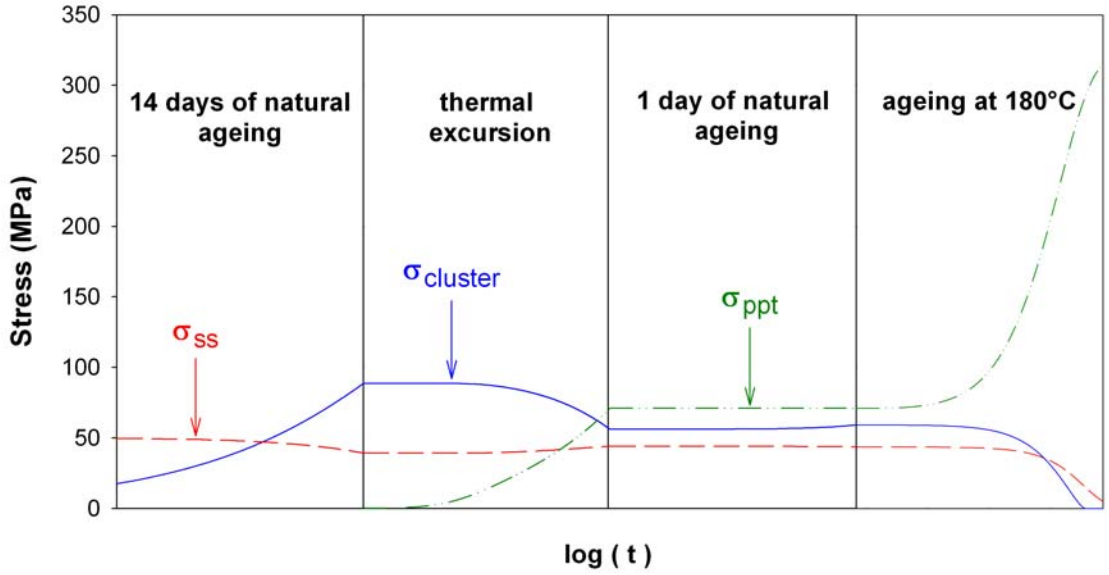

a)

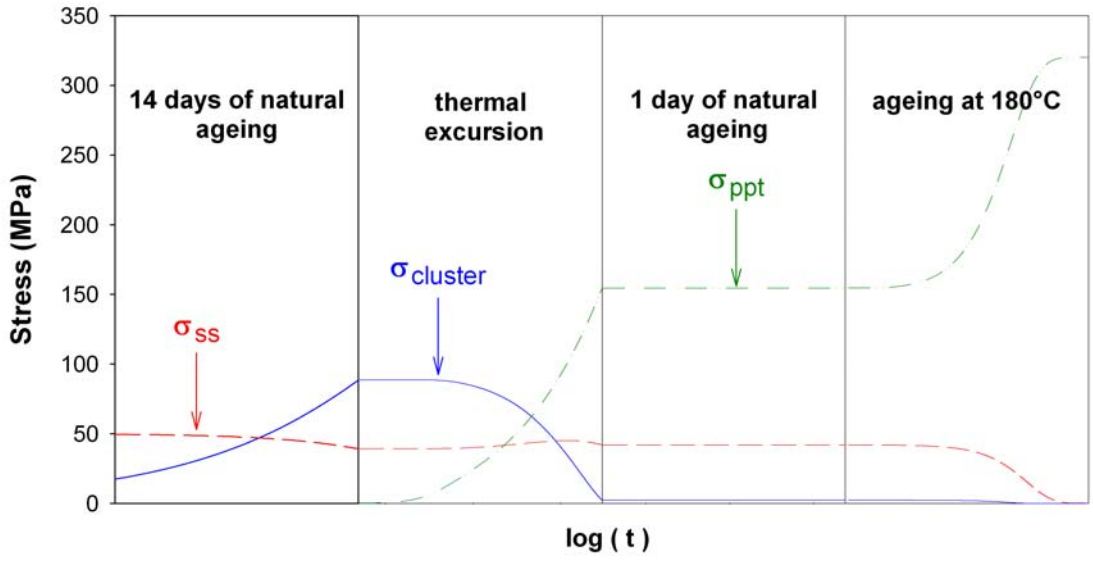

b)

Figure 5 – Model predictions for the evolution of the individual strengthen components as a function of time for the multi-step ageing treatment (Scenario B). a) thermal excursion time of 60 s and b) thermal excursion time of 300 s.

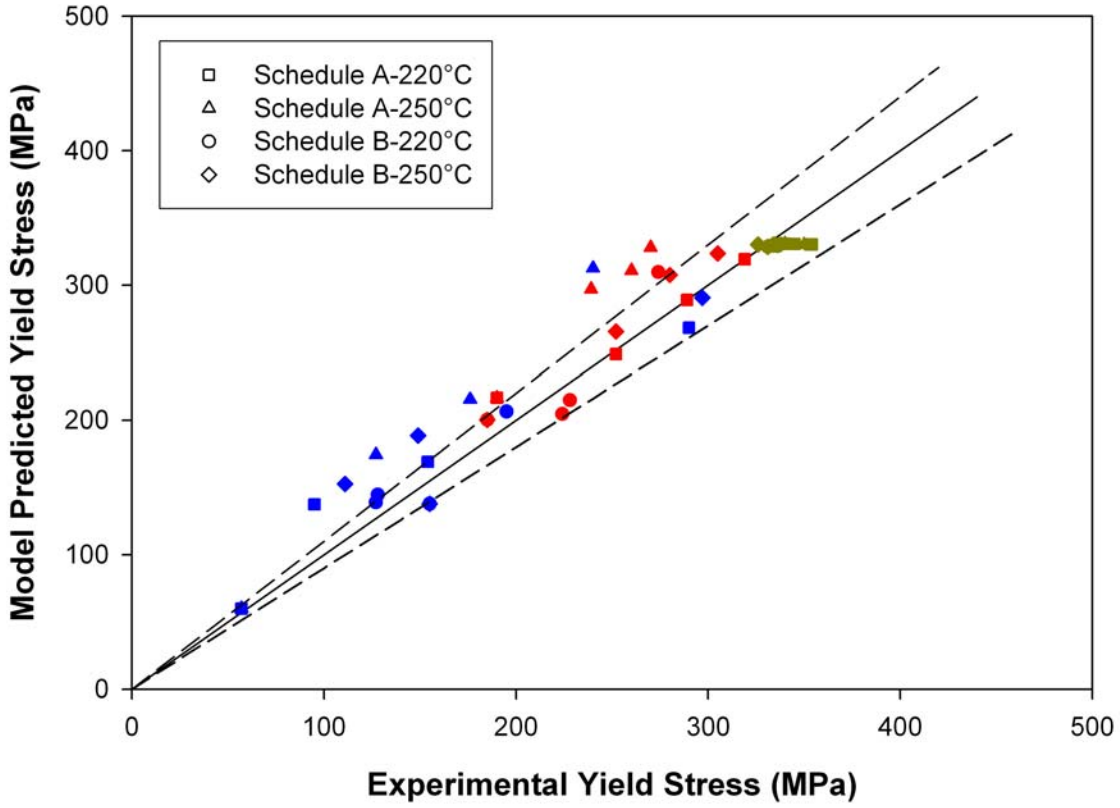

Figure 6 – A summary comparison of model predictions and experimental results for the yield stress of the alloy at very steps in the heat treatment, i.e. blue symbols refer to after thermal excursion, red symbols refer to after 30 minutes at 180 ^{o}C, and green symbosl refer to after 7 hours at 180 ^{o}C. Note dashed lines represent deviations of $\pm$ 10%.

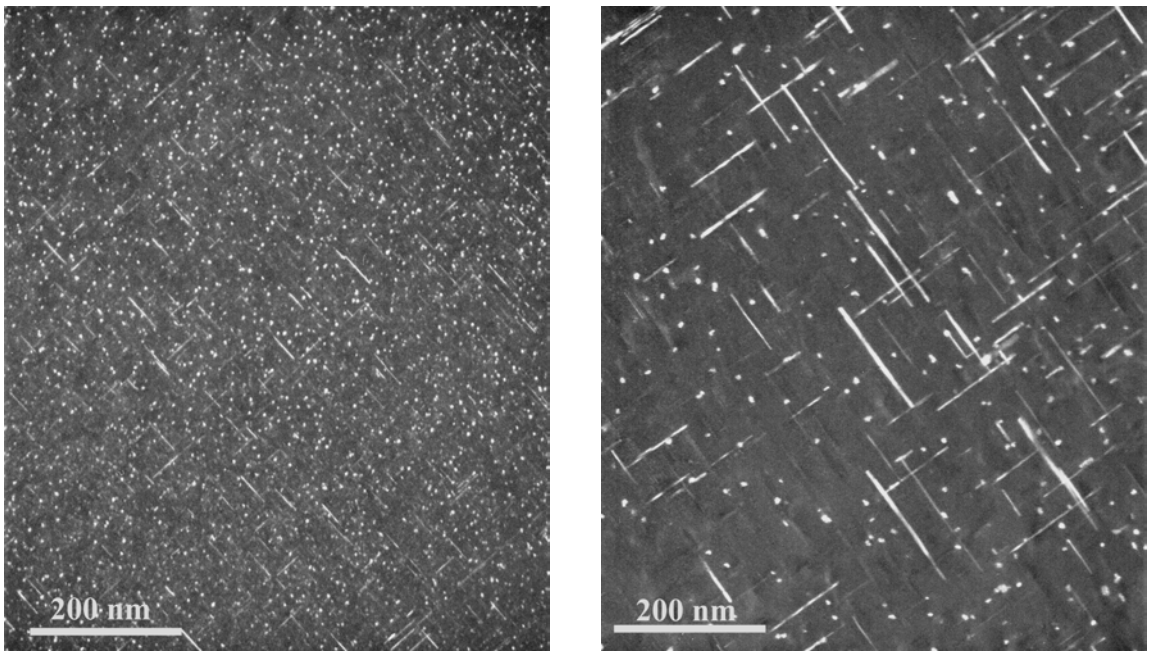

Figure 7 – Dark field TEM images illustrating the precipitate structure for material peak aged directly after the solution treatment at 180 and 250 ^{o}C, i.e. 7 hours and 30 minutes of ageing time, respectively. Note the much coarser structure for the material aged at 250 ^{o}C.